

Resonance-induced band gaps in a periodic waveguide

Zhi-Yong Tao*, Wei-Yu He, Xinlong Wang

Key Laboratory of Modern Acoustics and Institute of Acoustics, Nanjing University, Nanjing 210093, PR China

Received 20 March 2007; received in revised form 5 October 2007; accepted 30 November 2007

Handling Editor: L.G. Tham

Available online 22 January 2008

Abstract

The band gaps in periodic structures are usually regarded as being induced by the Bragg resonances. Until the recent years, the non-Bragg nature resonances were not taken into account in analysing and computing the band gaps, though it can exist in all kinds of waveguides with periodic structures. Here, the resonance-induced band gaps in a periodic acoustic duct are investigated extensively and a graphical method is introduced to analyse the dependence of these resonances on the duct geometry. With this method, it becomes quite easy to estimate the frequency band gaps of the waveguide and shape the band structures by choosing the proper geometric parameters. Our analysis show that the location and the width of the band gap are closely related to the wavenumber and the amplitude of the wall corrugations, and the non-Bragg resonance can result in the obvious band gap when the wall wavenumber is close to the cut-off frequency of the first mode. © 2007 Elsevier Ltd. All rights reserved.

1. Introduction

Wave propagation in periodic structures and media has attracted a broad interest of the researches in various branches of science for a long time, not only because of its fundamental importance in wave dynamics, but also of its vast application in engineering and technology [1,2]. The acoustical periodic structures, also known as phononic crystals, are bringing us more and more new concepts and methods, including the negative refraction and superlenses [3–5], thermal management [6], and so on. The classic work on acoustic period structures can be traced back as early as 1887 to Lord Rayleigh's study on one-dimensional wave propagation in a stretched string with periodically and continuously varying density. In that work, Rayleigh derived the governing equation of second order with periodic coefficient, and solved it by Hill's method [7]. Since the seventies of the last century, the developments of mathematical and computational techniques have greatly advanced the research on the periodic waveguides in acoustics and electromagnetics [8–22]. For instance, in 1974, Nayfeh [9] employed the method of multiple scales to find a uniform expansion near the sound resonances in a two-dimensional acoustic duct with small wall corrugations. With this method, he avoided the breaking down of the straightforward expansion, and showed that the resonance happened whenever the wall wavenumber was equal to the difference of the wavenumbers of any two duct acoustic modes and each of these two modes could not exit alone. Later, Bostrom [15] used the null-field method to find the stop-band structure

*Corresponding author.

E-mail address: zytao@nju.edu.cn (Z.-Y. Tao).

for the fundamental and the first modes in an axially symmetric hard-walled duct with a periodically varying cross section. In the 1990s, Bradley [17] investigated the linear, dissipative, time-harmonic acoustic waves in the periodic waveguide. In 2001, Wang [22] made a theoretical investigation on a periodically stubbed acoustic waveguide with the transfer-matrix method and obtained the tunable complete spectral gaps.

However, it should be pointed out that almost all of these researchers have paid their attention to the so-called Bragg resonance, and consequently, omitted the physical aspects in the sound frequency range far from the Bragg resonances. In fact, in that frequency range, the coupling of the transverse standing waves can result in the so-called non-Bragg resonance, which was predicted theoretically in our previous work [23]. Analogous resonant phenomenon in the planar electromagnetic waveguide was reported by Pogrebnnyak [24,25] before. Both Bragg and non-Bragg resonances in the acoustic waveguide are due to the interactions between the sound modes and the structural periodicity of the waveguide, which can be interpreted by the interferences of various wave modes in the waveguide and occur at the crossings of the different modes in the Brillouin zone. These resonances give rise to the generation of some new propagating modes and the formation of the so-called forbidden bands which can be found in such diverse areas as acoustics [26,27], optical superlattices [28], and the solid state physics [29,30]. Physically, band structures can result not only from the Bragg resonances but also from the non-Bragg resonances. However, one usually missed the physics due to non-Bragg resonance, especially in the numerical studies of band structures, and thus, he could not figure out the accurate relationship between the band structures and the waveguide parameters.

Moreover, ignoring the detailed spectral structures, we will miss more interesting applications. The band-gap engineering has already offered us some novel optical and electronic devices. Analogously, the analysis of acoustical band structures will help with the applications such as acoustic filters, noise control, and the improvements in the design of transducers. In 1996, Kushwaha computed the band structure of two-dimensional periodic arrays of rigid stainless steel cylinders in air and proposed the fabrication of a multiperiodic system in tandem that could create a huge hole in sound within the human audible range of frequencies [2]. In 2001, Lai proposed a simple, systematic, and efficient method to engineer acoustic band gaps and suggested the “designable” acoustic band gap for two-dimensional sonic crystals [31]. Rim [32], Auregan [33], Selamet [34,35], and many other authors have paid their attention to the noise control in the acoustic ducts for various applications. Some of them eliminated the noise by the resonance silencers, which prevent some sound wave elements from being transmitted through the ducts. Undoubtedly, the extensive analysis of the resonance-induced band gaps will benefit the design of it.

This paper is devoted to the Bragg and non-Bragg resonance-induced band gaps in the cylindrical acoustic duct with a periodically varying cross section. In the following section, the eigenvalue problem for the acoustic waves in the cylindrical duct is mentioned briefly and the generalized resonance conditions are derived. Section 3 introduces a graphical method to analyse the resonances and the frequency band structure (FBS) in the periodic waveguide. The numerical examples in Section 4 will confirm the analysis. The dispersion curves and band structures are given in the case of different duct parameters. And also, the attenuation properties are simulated with the finite element method. Section 5 summarizes the main results of the paper with a brief discussion.

2. Formulations

The theoretical formulation is summarized here in dimensionless form. For more details, reference should be made to our previous letter [23]. Assuming the harmonic wave motion in time, we obtain the dimensionless Helmholtz equation for the velocity potential ψ ,

$$\nabla^2\psi + \omega^2\psi = 0 \quad (1)$$

and the rigid boundary condition

$$\frac{\partial}{\partial \mathbf{n}}\psi = 0 \quad \text{on } r = 1 + \varepsilon \cos(kz), \quad (2)$$

where ω is the frequency, r the radius of the duct wall, ε a small parameter measuring the fluctuation of the wall, \mathbf{n} the outward unit vector normal to the wall and $2\pi/k$ the spacial period of the wall corrugations.

According to the Floquet’s theorem, the velocity potential ψ can be expanded in spatially harmonic series

$$\psi = \sum_{n=-\infty}^{\infty} A_n J_0(k_{r,n}r) e^{ik_{z,n}z}, \tag{3}$$

where $J_0(\cdot)$ is the zero-order Bessel function, $k_{z,n} = \beta + nk$ is the longitudinal wavenumber of the n th space harmonic, $\beta(-k/2 \leq \beta \leq k/2)$ is the reference propagation constant and $k_{r,n}$ is the transverse wavenumber. Also the dispersion relation,

$$\omega^2 = k_{r,n}^2 + k_{z,n}^2 \tag{4}$$

holds.

Substituting series (3) into the boundary condition (2) yields a system of linear algebraic equations for coefficients A_n , and then, whose determinant vanishes, i.e.

$$\det \|\mathbf{C}(k_{r,n}, \beta; \varepsilon, k)\| = 0, \tag{5}$$

where $\mathbf{C} = \{C_{mn}\}$ is an $m \times n$ matrix [23].

For a fixed frequency ω , the relation between the transverse wavenumbers of the n th and the n' th harmonics can be derived from the dispersion relation (4):

$$k_{r,n} = \sqrt{k_{r,n'}^2 + 2(n' - n)k\beta + (n'^2 - n^2)k^2}. \tag{6}$$

The resonance between the n th and n' th harmonics appears at

$$\beta_{pq} = -\frac{(n + n')k}{2}(1 + \eta_{pq}), \quad \eta_{pq} = \frac{k_r^{(q)2} - k_r^{(p)2}}{(n^2 - n'^2)k^2}, \tag{7}$$

where $k_r^{(p)}$ is the zeros of the first-order Bessel function, i.e. $\{k_r^{(p)}, p = 0, 1, 2, \dots\} = \{0, 3.8317, 7.0156, \dots\}$. The Bragg resonance appears as usual at $\beta = -(n + n')k/2$ when $p = q$, i.e., when both n th and n' th harmonics have the same transverse mode or radial distributions. Otherwise ($p \neq q$), the so-called non-Bragg resonance happens. Clearly it is a generalization of the Bragg resonance to the situations where different modes of non-propagated transverse standing waves are involved, even though the non-propagated waves do not couple with the periodic structures. The frequency of the generalized resonance between the p th mode of the n th harmonic and the q th mode of the n' th harmonic can be formulated as

$$\omega_{pq} = \sqrt{k_r^{(p)2} + (nk + \beta_{pq})^2} = \sqrt{k_r^{(q)2} + (n'k + \beta_{pq})^2}. \tag{8}$$

Near the resonance, Eq. (5) reduces to

$$k_{r,n'} J_1(k_{r,n'}) k_{r,n} J_1(k_{r,n}) = \varepsilon^{2|n-n'|} \frac{J_{nn'}^-(k_{r,n'}) J_{nn'}^+(k_{r,n})}{4} + O(\varepsilon^{3|n-n'|}), \tag{9}$$

where

$$J_{nn'}^\pm(k_{r,n}) = k_{r,n}^{(|n-n'|+1)} J_0^{(|n-n'|+1)}(k_{r,n}) \pm (n - n')k k_{z,n} k_{r,n}^{(|n-n'|-1)} J_0^{(|n-n'|-1)}(k_{r,n}). \tag{10}$$

In the above expression, $J_1(\cdot)$ is the first-order Bessel function and $J_0^{(m)}(\cdot)$ denotes the m th order derivative of $J_0(\cdot)$ with respect to the argument.

For small ε , we have the expansion,

$$k_{r,0} = k_r^{(p)} \pm \delta k_{pq} \varepsilon^{|n-n'|} \tag{11}$$

in terms of ε , with

$$\delta k_{pq} = \begin{cases} \frac{1}{2k_r^{(p)}} \sqrt{\frac{J_{nm'}^+(k_r^{(p)})J_{nm'}^-(k_r^{(q)})}{2J_1^{(1)}(k_r^{(p)})J_1^{(1)}(k_r^{(q)})}}, & q = 0, \\ \frac{1}{2k_r^{(p)}} \sqrt{\frac{J_{nm'}^+(k_r^{(p)})J_{nm'}^-(k_r^{(q)})}{J_1^{(1)}(k_r^{(p)})J_1^{(1)}(k_r^{(q)})}}, & q > 0. \end{cases} \quad (12)$$

Then, the frequency spectrum splits:

$$\omega_{pq}^\pm = \omega_{pq} \pm \frac{\omega^{(p)}}{\omega_{pq}} \delta k_{pq} \varepsilon^{|n-n'|}. \quad (13)$$

The resonance leads to the frequency shift and the generation of an additional mode ω_{pq}^- located away from the shifted frequency by

$$\Delta\omega_{pq} = 2 \frac{\omega^{(p)}}{\omega_{pq}} \delta k_{pq} \varepsilon^{|n-n'|}. \quad (14)$$

It is found that near the resonances, the spectral gap is proportional to $\varepsilon^{|n-n'|}$. When $|n - n'| = 1$, i.e., the resonance happens between two nearest spatial harmonics, the biggest splitting proportional to ε is obtained. This is the case considered in our previous letter [23].

3. Graphical method

To investigate the resonances and the relationship between the band gap and the wall periodicity of the waveguide, we introduce a graphical method in Fig. 1 according to the first equality in Eq. (8). The line marked by $l(p, n)$ in the figure denotes the p th mode of the n th harmonic. Also some special points are indicated. They are the cut-off frequencies of the first- and the second-mode $A(0, k_r^{(1)})$, $B(0, k_r^{(2)})$ and the intersections $M_0(0, k)$, $M_{-1}(-k/2, k/2)$, $M_1(k/2, k/2)$.

For the low-frequency sound waves ($\omega < k/2$), the solution to the wave equation is the linear combination of the right- and left-travelling sound waves. In the figure, the line $l(0, 0)$ stands for the two travelling waves. With the time harmonic $e^{-i\omega t}$, it stands for the right-travelling wave (RTW) when $\beta > 0$ and for the left one when $\beta < 0$. Because the wavelength is much greater than the period of the waveguide, the wall corrugations have no effect

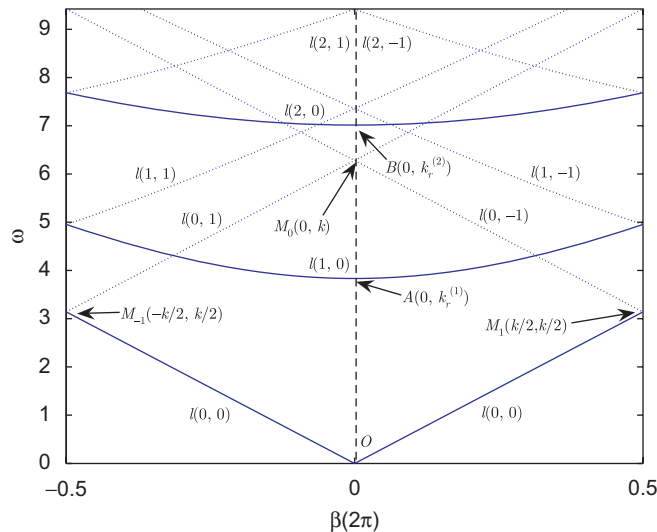


Fig. 1. The duct modes in the first Brillouin zone for $k = 2\pi$.

on the sound propagation, and the travelling is essentially the same as that in the straight duct. When the sound frequency ω is equal or close to $k/2$, i.e., under the Bragg reflection condition, the strongly reflected waves appear and interfere with the right- and left-travelling waves, respectively. At the point M_1 , the RTW interferes with the left-going reflected wave, resulting in the evanescent longitudinal standing wave. Analogously, at the point M_{-1} , the left travelling wave (LTW) interferes with the right-going reflected wave. In both cases, there is only the evanescent longitudinal standing wave left, and the wave energy attenuates very fast along the longitudinal direction. That is to say, the interferences give rise to the formation of the band gaps. When the frequency is away from $k/2$, the resonance condition is not satisfied any more. The right- and lefttravelling waves appear again, indicated by the line $l(0, 1)$ and $l(0, -1)$, respectively. When the frequency increases, more and more transverse modes will be involved. The cut-off frequencies of the first mode $k_r^{(1)}$ and the second $k_r^{(2)}$ are shown in Fig. 1 by points A and B , respectively. When the frequency gets a little larger than $k_r^{(1)}$, i.e., the frequency is near to the intersection of the lines $l(1, 0)$ and $l(0, 1)$ or $l(0, -1)$, the non-Bragg nature resonance occurs. For $\beta < 0$, the RTW of the fundamental mode interferes with the LTW of the first mode, and for $\beta > 0$, the LTW of the fundamental mode interferes with the RTW of the first mode. The constructive interferences lead to the frequency spectrum splitting, and the possibility of the band gap creation. Analogously, all the intersections in Fig. 1 stand for the resonances, which will result in the possible band gaps.

In the figure, the points M_0 , M_{-1} and M_1 depend on k , but the points A and B do not. When k gets small, the points M_0 , M_1 and M_{-1} move down. There will be no cut-off frequency in the parallelogram $OM_1M_0M_{-1}$ when $k < k_r^{(1)}$. For even smaller k , there will be more parallelograms under point A . When $k \ll k_r^{(1)}$, only the high-order spatial harmonics of the fundamental mode can intersect with the line $l(1, 0)$. Therefore, the non-Bragg resonances are too small to be observed and only the Bragg resonances dominate the bandgap formation. Fig. 2 shows the duct modes for $k = \pi/4$. The point M_0 is far away from the first-mode cut-off frequency and the Bragg resonances happen at the intersections in the figure. When $k > 2.709$, the non-Bragg resonances happen and result in the complete band gaps [23]. When k gets large, the points M_0 , M_1 and M_{-1} move up and more and more cut-off frequencies of the high-order modes go into the parallelogram $OM_1M_0M_{-1}$. The intersections of lines $l(0, \pm 1)$ and $l(p, 0)$ move to the line $\beta = \pm k/2$, and the Bragg and non-Bragg resonances have effect on each other. Fig. 3 shows the duct modes for $k = 3\pi$. Points A and B go into the parallelogram, and the non-Bragg nature resonances at the intersections between $l(1, 0)$ and $l(0, \pm 1)$ are moving to the line $\beta = \pm k/2$. When k gets even larger, the intersections between lines $l(1, 0)$ and $l(0, \pm 1)$ move up continuously. Although there is more spectrum splitting, the complete band gap can hardly be found because of the fixed points A , B , and so on.

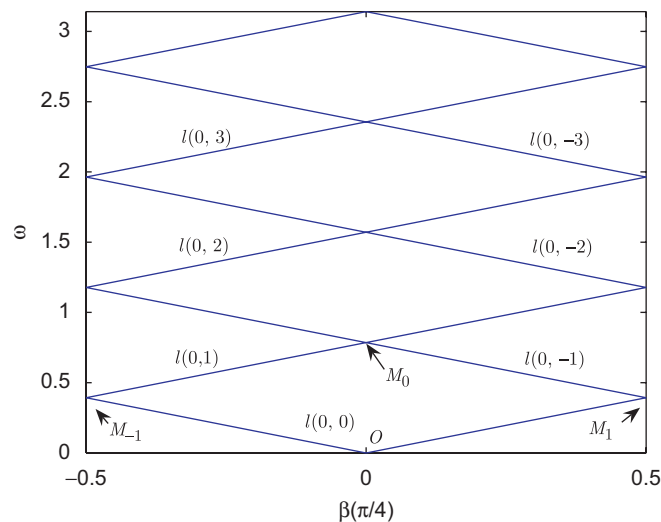


Fig. 2. The duct modes in the first Brillouin zone for $k = \pi/4$.

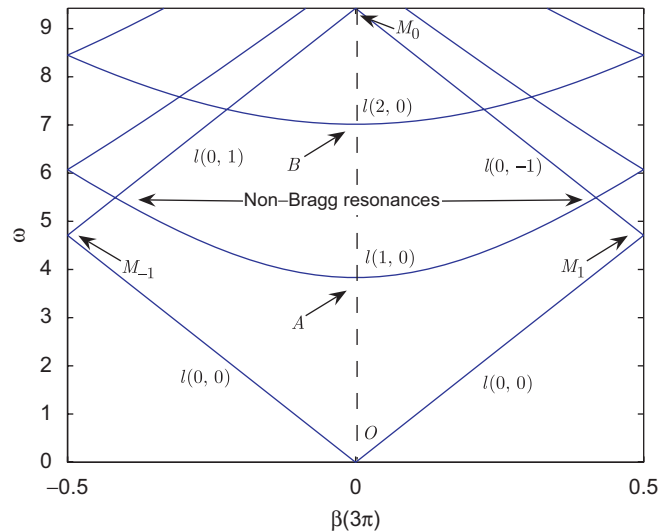


Fig. 3. The duct modes in the first Brillouin zone for $k = 3\pi$.

With the introduced graphical method, we can investigate how the resonances in the duct depend on the wall period. Thus, we can approximately estimate the FBS of a periodic waveguide. On the other hand, when a specific FBS is required in the application, we can design the geometric parameters of the waveguide with the help of the method. It is also possible to connect the different waveguides to broaden the band gaps in applications.

4. Numerical simulations

In the previous two sections, we have shown how the FBS in a periodic duct depend on the amplitude and the wavenumber of the wall corrugations, respectively. We also have demonstrated the power of the graphical method in facilitating the estimation and the designation of the waveguide qualitatively. For better understanding the relationship between the FBS and the wall parameters, numerical computation is given below to simulate the dispersion curves and the attenuation properties of the waveguide.

4.1. Dispersion curves

The dispersion curves can be calculated numerically based on Eq. (2). To achieve the goal, the infinite matrix in Eq. (5) must be truncated. The truncation depends on the order of the spatial harmonic considered. Generally, the 9×9 matrix ($-4 \leq m, n \leq 4$) gives the adequate approximation to the infinite system. The numerical results are shown in Figs. 4–6 for the first Brillouin zone, in comparison with the analytical ones in Figs. 1–3, respectively.

For $k = 2\pi, \varepsilon = 0.1$, Fig. 4 shows that the Bragg resonances occur near the line $\omega = \pi, 2\pi$. The resonances near the line $\omega = \pi$ can turn to the obvious band gap and those near the line $\omega = 2\pi$ have effect on the non-Bragg resonances. Also the non-Bragg resonances near the line $\omega = 4$ result in the complete band gap. Fig. 5 exhibits only the Bragg resonances because of the very small k . As we can see, the first-order Bragg resonance causes the widest band gap; the higher-order Bragg resonance, the narrower the band gap. In Fig. 6, not only the first and fundamental modes but also the second mode are included because of the frequency spectrum shifting with the larger ε [23]. The shifting also results in the superposition of the dispersive curves. So we can only find the non-Bragg band gap caused by the second-mode near the line $\omega = 6.5$, not by the first-mode. For very large k , Fig. 7 shows more modes involved, but no visible complete band gap.

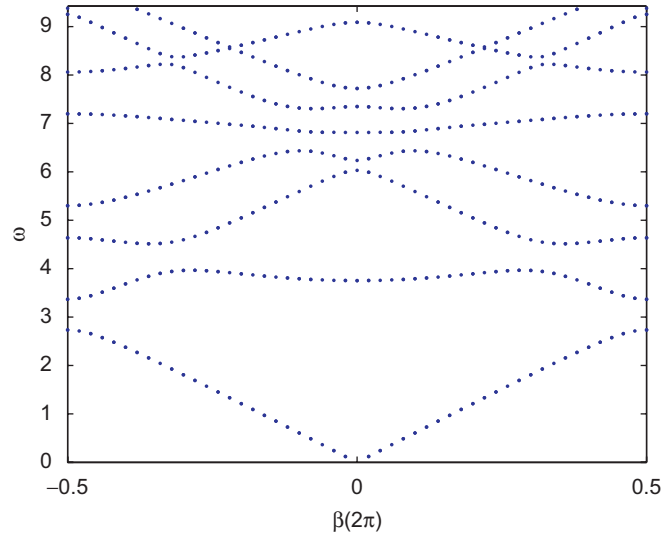


Fig. 4. The dispersion curves in the first Brillouin zone for $k = 2\pi, \epsilon = 0.1$.

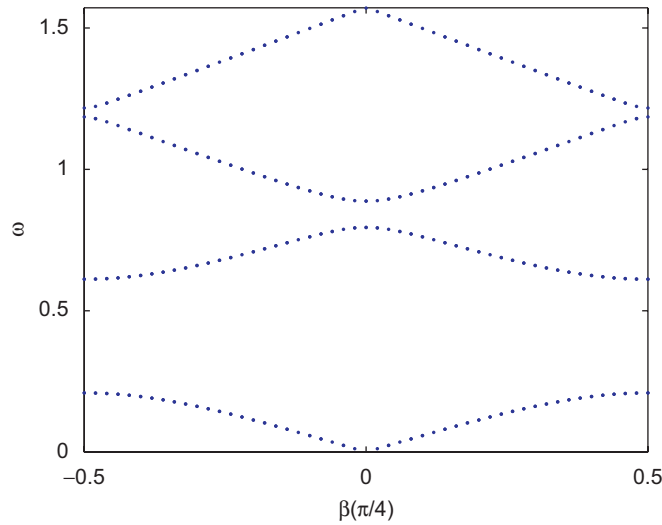


Fig. 5. The dispersion curves in the first Brillouin zone for $k = \pi/4, \epsilon = 0.5$.

4.2. Attenuation properties

With the finite element method, the attenuation properties of the waveguide with 20 periods are investigated and the results confirm the previous analysis. We take the plane wave as the incident wave of the sound power p_{in} at one end and calculate the output power p_{out} at the other end of the waveguide. Defining the power attenuation as

$$p = 10 \log_{10} \frac{p_{out}}{p_{in}} \tag{15}$$

we obtain the attenuation properties as shown in Figs. 8–11. All the attenuations in the figures correspond to the resonances predicted above. With the help of the graphical method or the dispersion curves described above, we can easily recognize the Bragg or the non-Bragg resonances in these figures. For example, the band

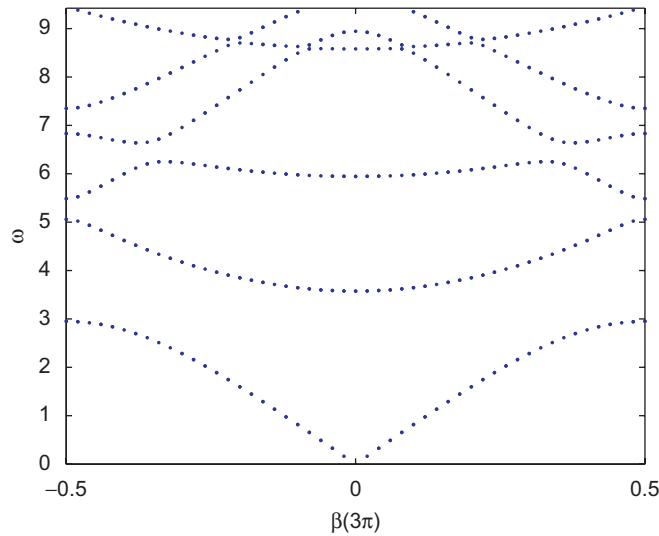


Fig. 6. The dispersion curves in the first Brillouin zone for $k = 3\pi, \varepsilon = 0.2$.

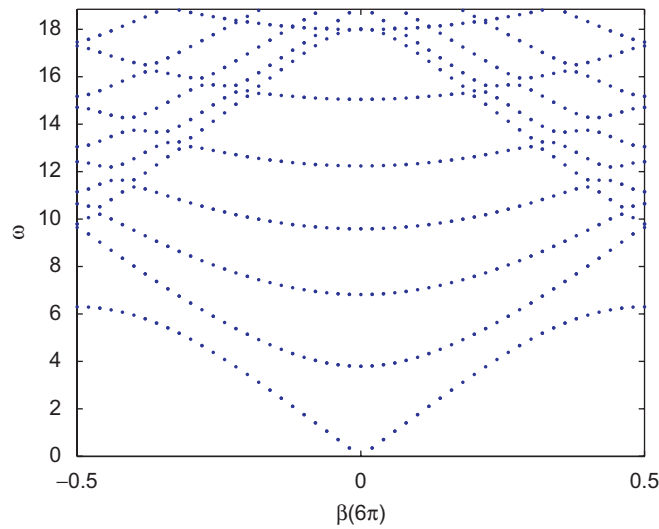


Fig. 7. The dispersion curves in the first Brillouin zone for $k = 6\pi, \varepsilon = 0.1$.

gap near the line $\omega = 4$ in Fig. 8 and that near the line $\omega = 6.5$ in Fig. 10 are the obvious non-Bragg induced ones. Fig. 11 shows no band gap in the frequency range considered, in agreement with the prediction in Fig. 7.

5. Discussion and conclusion

In this paper, the FBS of the acoustic cylindrical duct with sinusoidally corrugated wall is investigated. Not only the Bragg resonance but also the non-Bragg resonance appear to result in the gaps. The non-Bragg resonance is caused by the interaction between the transverse standing wave modes, while the well-known Bragg resonance is due to the interaction of the longitudinal wave modes. Because of the non-Bragg resonance, some new forbidden bands appear in addition to those due to the Bragg resonance. In other words, the non-Bragg resonance becomes important for k large enough to introduce the high-order modes. Both the Bragg and non-Bragg resonance conditions are formulated in a unified way, and the spectrum splits are

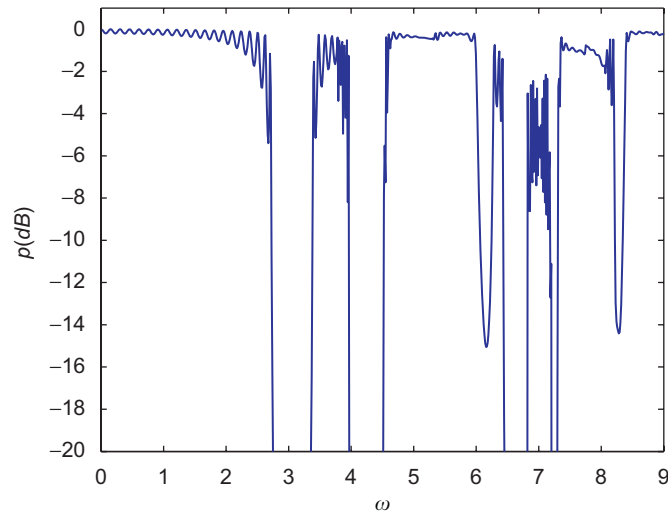


Fig. 8. The power attenuation at the end of the waveguide for $k = 2\pi, \varepsilon = 0.1$.

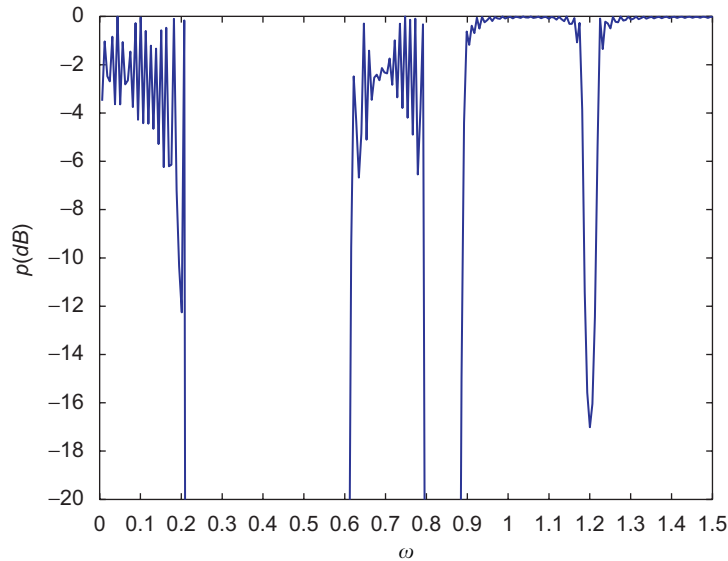


Fig. 9. The power attenuation at the end of the waveguide for $k = \pi/4, \varepsilon = 0.5$.

predicted theoretically. The qualitative and quantitative analysis are performed to enrich our knowledge on periodic waveguides. The main results can be summarized as

- (1) When $k \ll k_r^{(1)}$, only the Bragg nature resonances are involved, and the band gaps appear near $\omega = |(n + n')k/2|$.
- (2) When $k_r^{(1)}/k = O(1)$, the non-Bragg nature resonances caused by the first-order mode, can result in the obvious band gaps.
- (3) When $k \gg k_r^{(1)}$, more and more transverse modes are involved, and no complete band gap can be found.

The theoretical and numerical results show that the resonance between two nearest spatial harmonics leads to the widest spectrum stop band. The resonance-induced band structures are found to depend highly on the wall parameters, i.e., the location and width of the band gap is closely related to the wall wavenumber and

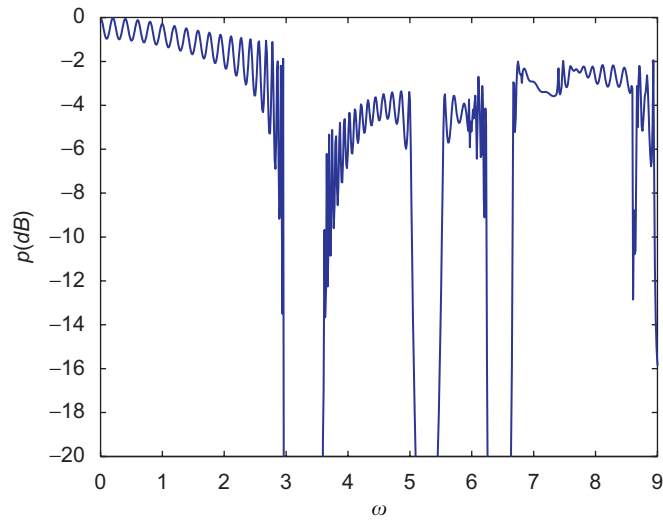


Fig. 10. The power attenuation at the end of the waveguide for $k = 3\pi$, $\varepsilon = 0.2$.

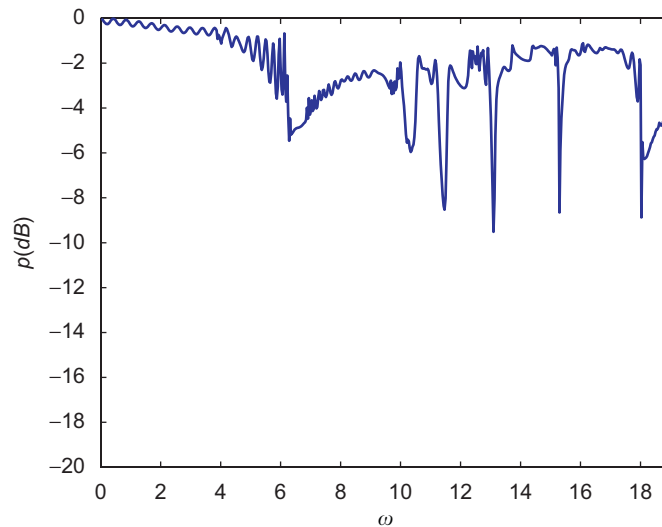


Fig. 11. The power attenuation at the end of the waveguide for $k = 6\pi$, $\varepsilon = 0.1$.

amplitude. The proposed graphical method greatly help us to analyse the band structure of the duct qualitatively. It also makes it possible to design some special band structures with the compound waveguides consisting of different wall periods. We believe that the present work might provide a clearer picture of physics of sound wave interactions and propagation in periodic waveguide. Further theoretical and experimental researches with regard to the “band-gap design” are still underway.

Acknowledgements

The authors would like to thank the reviewers for their helpful suggestions. This work is supported by the National Science Foundation of China under Grant Nos. 10474045, 10604031, and the Research Fund for the Doctoral Program of Higher Education of China under Grant no. 20050284018.

References

- [1] L. Brillouin, *Wave Propagation in Periodic Structures*, Dover, New York, 1953.
- [2] M.S. Kushwaha, Classical band structure of periodic elastic composites, *International Journal of Modern Physics B* 10 (1996) 977–1094.
- [3] X. Zhang, Z. Liu, Negative refraction of acoustic waves in two-dimensional phononic crystals, *Applied Physics Letters* 85 (2004) 341–343.
- [4] L. Feng, et al., Negative refraction of acoustic waves in two-dimensional sonic crystals, *Physical Review B* 72 (2005) 033108.
- [5] L. Feng, et al., Acoustic backward-wave negative refractions in the second band of a sonic crystal, *Physical Review Letters* 96 (2006) 014301.
- [6] T. Gorishnyy, C.K. Ullal, M. Maldovan, G. Fytas, E.L. Thomas, Hypersonic phononic crystals, *Physical Review Letters* 94 (2005) 115501.
- [7] L. Rayleigh, On the maintenance of vibrations by forces of double frequency and on the propagation of waves through a medium endowed with a periodic structure, *Philosophical Magazine* XXIV (1887) 145–159.
- [8] R.F. Salant, Acoustic propagation in waveguides with sinusoidal walls, *Journal of the Acoustical Society of America* 53 (1973) 504–507.
- [9] A.H. Nayfeh, Sound waves in two-dimensional ducts with sinusoidal walls, *Journal of the Acoustical Society of America* 56 (1974) 768–770.
- [10] O.R. Asfar, A.H. Nayfeh, Circular waveguide with sinusoidally perturbed walls, *IEEE Transactions on Microwave Theory and Techniques* 23 (1975) 728–734.
- [11] A.H. Nayfeh, Acoustic waves in ducts with sinusoidally perturbed walls and mean flow, *Journal of the Acoustical Society of America* 57 (1975) 1036–1039.
- [12] A.H. Nayfeh, O.A. Kandil, Propagation of waves in cylindrical hard-walled ducts with generally weak undulations, *AIAA Journal* 16 (1978) 1041–1045.
- [13] O.R. Asfar, A.H. Nayfeh, Stopbands of the first-order Bragg interaction in a parallel-plate waveguide having multiperiodic wall corrugations, *IEEE Transactions on Microwave Theory and Techniques* 28 (1980) 1187–1191.
- [14] S.A. Kheifets, Electromagnetic fields in an axial symmetric waveguide with variable cross section, *IEEE Transactions on Microwave Theory and Techniques* 29 (1981) 222–229.
- [15] A. Bostrom, Acoustic waves in a cylindrical duct with periodically varying cross section, *Wave Motion* 5 (1983) 59–67.
- [16] S. Sandstrom, Stopbands in a corrugated parallel plate waveguide, *Journal of the Acoustical Society of America* 79 (1986) 1293–1298.
- [17] C.E. Bradley, Time harmonic acoustic Bloch wave propagation in periodic waveguides. Part I. Theory, *Journal of the Acoustical Society of America* 96 (1994) 1844–1853.
- [18] M.A. Hawwa, Acoustic/elastic stop-band interaction in waveguides involving two periodicities, *Journal of the Acoustical Society of America* 102 (1997) 137–142.
- [19] J.N. Munday, C.B. Bennett, W.M. Robertson, Band gaps and defect modes in periodically structured waveguides, *Journal of the Acoustical Society of America* 112 (2002) 1353–1358.
- [20] A. Morales, J. Flores, L. Gutierrez, R.A. Mendez-Sanchez, Compressional and torsional wave amplitudes in rods with periodic structures, *Journal of the Acoustical Society of America* 112 (2002) 1961–1967.
- [21] J.J. Barroso, J.P. Leite Neto, K.G. Kostov, Examining by the Rayleigh–Fourier method the cylindrical waveguide with axially rippled wall, *IEEE Transactions on Plasma Science* 31 (2003) 752–764.
- [22] X.F. Wang, M.S. Kushwaha, P. Vasilopoulos, Tunability of acoustic spectral gaps and transmission in periodically stubbed waveguides, *Physical Review B* 65 (2001) 035107.
- [23] Z.Y. Tao, Y.M. Xiao, X.L. Wang, Non-Bragg resonance of standing acoustic wave in a cylindrical waveguide with sinusoidally perturbed walls, *Chinese Physics Letters* 22 (2005) 394–397.
- [24] V.A. Pogrebnnyak, Geometric resonance in a periodic waveguide, *Journal of Applied Physics* 94 (2003) 6979–6981.
- [25] V.A. Pogrebnnyak, Non-Bragg reflections in a periodic waveguide, *Optics Communications* 232 (2004) 201–207.
- [26] T.T. Wu, Z.G. Huang, Level repulsions of bulk acoustic waves in composite materials, *Physical Review B* 70 (2004) 214304.
- [27] T.T. Wu, Z.G. Huang, S.C. Lin, Surface and bulk acoustic waves in 2D phononic crystals consisting of materials with general anisotropy, *Physical Review B* 69 (2004) 94301.
- [28] P.St.J. Russell, Bragg resonance of light in optical superlattices, *Physical Review Letters* 56 (1986) 596–599.
- [29] Y. Takagi, K. Kusakabe, Transition from direct band gap to indirect band gap in fluorinated carbon, *Physical Review B* 65 (2002) 121103.
- [30] S.V. Dudiy, A. Zunger, M. Felici, A. Polimeni, M. Capizzi, H.P. Xin, C.W. Tu, Nitrogen-induced perturbation of the valence band states in GaP_{1-x}N_x alloys, *Physical Review B* 74 (2006) 155303.
- [31] Y. Lai, X.D. Zhang, Z.Q. Zhang, Engineering acoustic band gaps, *Applied Physics Letters* 79 (2001) 3224–3226.
- [32] M. Rim, Y. Kim, Narrowband noise attenuation characteristics of in-duct acoustic screens, *Journal of Sound and Vibration* 234 (2000) 737–759.
- [33] Y. Auregan, A. Debray, R. Starobinski, Low frequency sound propagation in a coaxial cylindrical duct: application to sudden area expansions and to dissipative silencers, *Journal of Sound and Vibration* 243 (2001) 461–473.
- [34] A. Selamet, M.B. Xu, I.J. Lee, N.T. Huff, Helmholtz resonator lined with absorbing material, *Journal of the Acoustical Society of America* 117 (2005) 725–733.
- [35] A. Selamet, M.B. Xu, I.J. Lee, N.T. Huff, Analytical approach for sound attenuation in perforated dissipative silencers with inlet/outlet extensions, *Journal of the Acoustical Society of America* 117 (2005) 2078–2089.